Research Article

Journal of RAMAN SPECTROSCOPY

Received: 2 January 2012 Accepted: 2 January 2012 Published online in Wiley Online Library: 27 April 2012

(wileyonlinelibrary.com) DOI 10.1002/jrs.3171

CARS and SHG microscopy to follow collagen production in living human corneal fibroblasts and mesenchymal stem cells in fibrin hydrogel 3D cultures†

L. Mortati, C. Divieto and M. P. Sassi*

Coherent anti-Stokes Raman scattering (CARS) microscopy is used in conjunction with second harmonic generation (SHG) to follow the early stage of stem cell differentiation within a three-dimensional (3D) scaffold. Formation of an extracellular matrix mainly composed of collagen is one of the first signs of human mesenchymal stem cell (hMSC) differentiation. This work shows that the multimodal CARS and SHG constitutes a powerful noninvasive, label-free technique for monitoring collagen production in 3D cell cultures. Its simultaneous imaging of cell morphology and the distribution of the collagen produced by living cells during long-term (4 weeks) experiment furnished important information about the cell-scaffold interaction and the establishment of the extracellular matrix, while its very low collagen detection limit permitted mapping of even the small quantity produced in a few hours. This finding indicates that the multimodal CARS and SHG imaging can be proposed as a new way of monitoring the differentiation of stem cells by evaluating their production of collagen in both short and long-term experiments. Further evidence is also provided of the efficacy of fibrin hydrogel as a scaffold autoinducing the differentiation stimulus in 3D human mesenchymal stem cell cultures. Copyright © 2012 John Wiley & Sons, Ltd.

Keywords: CARS; SHG microscopy; mesenchymal stem cell; fibrin hydrogel; collagen

Introduction

Regenerative medicine uses biomimetic materials (scaffolds) and cells to facilitate regeneration of tissues and organs *in vivo*.[1–3] Mesenchymal stem cells (MSCs) have been widely investigated in the last 20 years in *in vitro* studies for regenerative medicine applications[3] because of their role to maintain the cell natural turnover, replacing differentiated cells naturally expired or damaged/dead because of an injury or a disease.[4,5] MSCs, isolated from the bone marrow aspirates or from adipose tissue, umbilical cord blood or placenta,[6,7] can be cultured *in vitro* and can be induced to differentiate in several cell types, such as bone, cartilage, tendon, cardiac muscle, skeletal muscle, neural cells, adipose and connective tissue.[3,4,8,9] The biomimetic scaffolds offer to MSCs the native physiologic-like and three-dimensional (3D) environment that surrounds *in vivo* tissues and organs.[3] Recent studies showed that scaffold chemical composition, internal architecture and stiffness are parameters of influence for the behaviour and functions of the cells seeded on it.[10–12] This makes extremely important the study of interactions between scaffold and stem cells *in vitro* before implanting the cell-scaffold construct.

In their native environment, stem cells are surrounded by a 3D extracellular matrix (ECM) produced by fibroblasts. ECM is involved in regulating cell behaviour (e.g. survival and proliferation) and function (e.g. differentiation) and it is composed by several proteins and other macromolecules. Collagen is the main ECM component and the most abundant protein in mammals and it gives a mesh structure to the ECM.[13,14] In stem cell biology, it is well known that MSCs cultured *in vitro* can differentiate producing ECM when chemically or mechanically stimulated.[9,15–17]

Collagen production represents one of the first steps of ECM formation[14] and it is normally assessed *in vitro* as an indicator of cell differentiation process.[18–20] Collagen shows a noncentrosymmetric ordered triple-helix structure with a very high level of crystallinity, which is a suitable condition for enabling second harmonic generation (SHG) process.[21] Stem cell behaviour can be studied through their morphology changes, thus their membrane image is a suitable tool for cell behaviour studies in interaction with scaffolds. CARS microscopy, providing chemical contrast from Raman-active CH_2 symmetric stretching vibration wavenumber at around 2845 cm^{-1}, provides high contrast membranes morphology.

The dynamics of collagen production can be studied as a biomarker of cell differentiation with several techniques. However, conventional techniques are destructive and/or invasive, require manipulation of the cells, do not provide information about spatial distribution of the protein: gene expression analysis contemplates destructive procedure steps and loses the spatial distribution of the protein; western blot protein analysis needs to destroy samples and requires a consistent amount of protein;

* *Correspondence to: M. P. Sassi, INRIM - Istituto Nazionale di Ricerca Metrologica, Strada delle cacce, 91 – 10135 Torino, Italy. E-mail: m.sassi@inrim.it*

† *This article is part of the Journal of Raman Spectroscopy special issue entitled "Development and applications of nonlinear optical spectroscopy - 10th ECONOS / 30th ECW meeting in Enschede, The Netherlands" edited by Herman Offerhaus, Peter Radi, and Cees Otto.*

INRIM - Istituto Nazionale di Ricerca Metrologica, Strada delle cacce, 91 – 10135 Torino, (Italy)

immunofluorescence techniques for protein analysis give information on the spatial distribution of the protein but samples need to be fixed and/or sectioned. Moreover, traditional techniques are unable to follow, in nondestructively short and long term experiments, the dynamic distribution of collagen produced from the same sample.

A nondestructive and noninvasive procedure based on CARS and SHG combined microscopy, able to investigate the cell-scaffold interaction in terms of cell behaviour and functions over the time is discussed in this work. The aim is to demonstrate that a combined CARS and SHG microscopy is an adequate and optimal technique to follow on different time scales the collagen produced by cells cultured in a 3D scaffold, with a noninvasive, nondestructive and label-free method.

The collagen produced by living human corneal fibroblasts (hCFs) and human mesenchymal stem cells (hMSCs) seeded in a fibrin hydrogel matrix has been monitored over time. Fibrin hydrogel is largely used in regenerative medicine as a biodegradable, biocompatible and noncytotoxic scaffold, capable of inducing both osteogenic and chondrogenic stem cell differentiation.[22,23] This scaffold is known to support and to stimulate, through its composition and stiffness, in absence of any external chemical and mechanical stimulus, stem cells differentiation with collagen production.[24] hCFs have been chosen as positive control for collagen production because they are normally devoted to produce collagen *in vivo* and they maintain this property also when cultured *in vitro*.[5,25,26] hMSCs have been chosen to investigate the fibrin hydrogel capability to induce stem cells collagen production without any other kind of stimuli. Multiphoton microscopy based on the combination of multiple nonlinear optical phenomena like CARS and SHG,[27] allows deep tissue penetration[28] and high 3D spatial resolution,[29] that are powerful requirements in analyzing thick tissue sections at cellular level. CARS microscopy provides chemical contrast from Raman-active molecular vibrations and it is able to detect membranes and lipid droplet compartments in living cells, like fibroblasts[30,31] tuning the excitation sources to the CH2 symmetric stretching vibration wavenumber at around 2845 cm-1. SHG microscopy is based on a second order nonlinear optical process and it is sensitive to the molecular structures, enabling a strong imaging contrast for non-centrosymmetric molecular ordered structures such as collagen,[32–37] microtubule arrays,[38] skeletal muscle myosin,[39,40] cell membranes,[41] and also cellulose.[42] Recently it has been demonstrated that CARS and SHG techniques can be easily combined together in the same microscopy allowing multiple chemical contrasts.[43–46]

Coherent anti-Stokes Raman scattering and SHG techniques have been combined in the same microscope to follow in time the same living cells sample into a 3D scaffold in a four week experiment. CARS were used to image living cells morphology and SHG to detect the collagen formation.

Experimental

CARS and SHG microscopy

A passively mode-locked Nd : YVO_4 (Yttrium Vanadate crystal doped with Neodymium) laser emitting at 1064 nm (Picotrain, HighQLaser) was used as a master source for CARS and SHG microscopy. This optical source emits a continuous train of 10 ps pulses at the repetition rate of 76 MHz and it is equipped with an SHG unit. The 532 nm output of the SHG frequency doubling has a pulse width of about 5 ps and it is used to synchronously pump an optical parametric oscillator (OPO) (Levante Emerald, APE Berlin). The OPO acts as the tuneable source and it is based on a nonlinear lithium–triborate (LBO, LiB_3O_5) crystal as a parametric amplifier in a resonant optical cavity. The tuning range is 700 to 1020 nm for the signal wave and 1110 to 2200 nm for the idler wave. Signal and idler beams exit collinear in our experiments, entering the scanning unit (FluoView FV300, Olympus) combined with an upright microscope (BX51WI, Olympus). This allows a point-by-point detection of CARS and SHG signals all over the sample with high resolution and high excitation efficiency. The *Z* depth scanning is achieved by moving the focusing objective with a stepping motor.

To focus the excitation beams on living cells samples, a water immersion objective (LUMPLFLN 60XW NA = 1 W.D. = 2 mm, Olympus), fully compensating for both spherical and chromatic aberrations from the UV to the near infrared region, was used. The water immersion objective was cleaned and sterilized with a solution 70% ethanol in water (v/v) before each imaging experiment to prevent cell culture damages.

The forward descanned CARS and SHG signals are collected through an objective (UPLSAPO 20× objective NA = 0.75 W. D. = 0.6 mm, Olympus) and focused on a PMT (R3896, Hamamatsu) with a plano-convex lens with a focal length 25 mm.

Cell membrane structures were imaged using CARS process looking at the CH_2 symmetric stretch Raman modes around 2844 cm^{-1}. The CARS signal was generated around 731.8 nm by tuning the pump and the Stokes beams to 924.1 and 1253.7 nm, respectively.

Collagen structures were imaged using SHG process, tuning the OPO signal to 950 nm and detecting the corresponding SHG wavelength at 475 nm.

To further block the residual excitation beams and transmit the CARS and the SHG signals respectively, bandpass filters centered at 716 nm with 43 nm bandwidth (FF01-716/43, Semrock) and at 480 nm with 20 nm bandwidth (BP470-490, Chroma Technology), both coupled with shortpass filters with 770 nm of cut-off wavelength (FF01-770/SP, Semrock), are placed before the detector.

To prevent sample damages and optimize the output signal, the excitation beams were attenuated through a neutral density variable filter wheel (NDC-50 C-4 M, Thorlabs).

FluoView FV300 Olympus software was used to acquire the images; the acquisition speed was about 9 μs/pixel. SHG images were processed using ImageJ software to enhance their contrast; a detection limit enhancement (0.4% of saturate pixels with histogram equalization) followed by a Gaussian blurring (one pixel size) and a manual adjustment of the brightness/contrast levels were performed, lowering the detection limit of collagen beyond 0.01 mg/mL.

Coherent anti-Stokes Raman scattering and SHG imaging are obtained on the same sample in sequence for a total observation time ranging between 10 and 20 min. This time is negligible with respect to the characteristic time of the collagen production process and of the dynamic of a cell in the fibrin hydrogel, allowing to assume a simultaneous observation of the cell morphology and of the produced collagen distribution.

Coherent anti-Stokes Raman scattering microscopy at 2844 cm^{-1} was performed in three dimensions at *Z*-axis steps of about 800 nm. The overall *Z* scan range was chosen

Journal of RAMAN SPECTROSCOPY

accordingly to the 3D extension of the cells in the fibrin hydrogel. The *XY* pixel pitch was equal to 0.230178 μm/pixel for all the measurements, while the image size was adapted according to cells shape in each experiment. The overall 3D imaging lasted between 5 and 10 min according to the *Z* scan range, and for each *Z*-step up to nine images were acquired and adaptively averaged using a Kalman filter.

Pixel dwell time was 9.1 μs and the average power at the sample was about 25 mW for the pump signal and less than 10 mW for Stokes signal. The slices obtained for each experiment were used to create a maximum intensity *Z*-projection image to have in a single picture all the interesting extension of the cell in the measured volume.

Collagen detection was performed using SHG microscopy technique after CARS imaging, keeping the same dimensional and temporal parameters of the related CARS imaging. The average excitation power at the sample was about 20 mW.

A maximum intensity *Z*-projection was made also for SHG imaged slices, obtaining a single picture of the measured volume. SHG *Z*-projected images were processed using ImageJ software contrast enhancement followed by a Gaussian blurring with one pixel size and a manual brightness/contrast adjustment. After these operations, the SHG intensity image became a quasi-binary image, holding all the information related to the collagen distribution in a clearer manner.

Cell selection and culture in fibrin gel scaffolds

Human mesenchymal stem cells were purchased from Lonza (Basel, Switzerland). They are bone marrow derived-hMSCs from a donor. They were expanded and maintained in a complete non-differentiating growth medium (MSCBM, Lonza) supplemented with 10% fetal bovine serum (FBS), 2% L-glutamine, 0,1% antibiotics (gentamicin and amphotericin B) (Lonza).

Human corneal fibroblasts were kindly provided by Dr Sizzano (Transplants Centre of the Regione Piemonte). hCFs were expanded, maintained and resuspended in Dulbecco's Modified Eagle Medium (DMEM) (Listarfish, Milano, Italy) containing 10% FBS, 1% L-Glutamine and 1% kanamycin. Cells were cultured until they reached 80–85% of confluency (cells surface per total area), then they were washed with 1× phosphate buffer saline (PBS), detached with 0.05% trypsin/0.53 mM Ethylenediaminetetraacetic acid (EDTA), counted by means of a hemocytometer and suspended at 1×10^6 cells per 200 μL complete growth medium to be seeded within the scaffolds of fibrin gel. hMSCs were used at passage 8 and hCFs at passage 10 to prepare the fibrin gel and cells constructs.

Scaffolds of fibrin gel preparation

Fibrin gel scaffolds were prepared from fibrinogen and thrombin, both proteins involved in blood clotting. Fibrinogen (5 mg/mL) (Sigma, USA; Cat #.F8630) was reconstituted in PBS 1× and thrombin (25 ug/mL) (Sigma, USA; Cat #. T9549) was reconstituted in PBS 1×. 3D fibrin scaffolds containing cells were prepared in 35×10 mm cell culture dishes (CytoOne) by mixing in the following order: 325 μL of thrombin (25 ug/mL), 125 μL of medium, 200 μL of cell suspension, 1350 μL of fibrinogen (5 mg/mL). The components were allowed to polymerize undisturbed at room temperature for 5 min to obtain fibrin 3D scaffolds with thickness of about 4 mm. Then the scaffolds were covered with 2 mL of cell culture medium and placed in an incubator for cell cultures under controlled conditions of temperature (37 °C) and CO_2 (5%). Cells within the scaffolds were fed every 3–4 days by completely replacing the medium with fresh medium. Five samples were prepared for both cell types to be able to detect the collagen production at days 0, 7, 14, 21, 28 even in case of culture damage because of the measurement procedure.

Results and Discussion

Three-dimensional CARS imaging of living hCF and hMSC cells, cultured in a 4-mm-thick fibrin hydrogel scaffolds, was conducted in time-course experiment at different days in culture (day 0, 7, 14, 21, 28); in the same way the collagen produced by the same cells was detected and imaged using the second harmonic signal generated by the collagen itself.

Different tests were made to demonstrate (a) the second harmonic signal as generated by collagen, (b) the absence of interfering and spurious autofluorescent signals possibly coming from the scaffold and from the samples and (c) the CARS signal generated by the weak Raman-active band around 2844 cm^{-1} of fibrin hydrogel does not impair the contrast ability for an high resolution cell morphology analysis.

Figure 1 shows the result obtained by CARS and SHG imaging a fibrin hydrogel scaffold spiked with 1 mg/mL of rat tail type I collagen. It is evident the second harmonic signal generated from collagen (white) while it is slightly visible a very weak CARS signal arising from fibrin hydrogel (red).

For every measurement, cells to be imaged have been chosen in the thick scaffold, selecting those being in the fibrin matrix region with a midlevel confluency (40% –50%). A comparison between hCFs and hMSCs collagen production over time was performed, where hCFs represent the positive control for collagen production while the hMSCs allow a measurement of the fibrin hydrogel capability to induce stem cells collagen production without any other kind of stimuli. Even if submitted to subsequent measurements, cells in the fibrin gel were not contaminated, continuing to proliferate in culture. This is a further proof of using a noninvasive technique that does not induce any relevant influence on cell growth, thus allowing very interesting studies in unperturbed conditions.

Figure 2 reports the results obtained respectively at culture days 0, 7, 14, 21, 28.

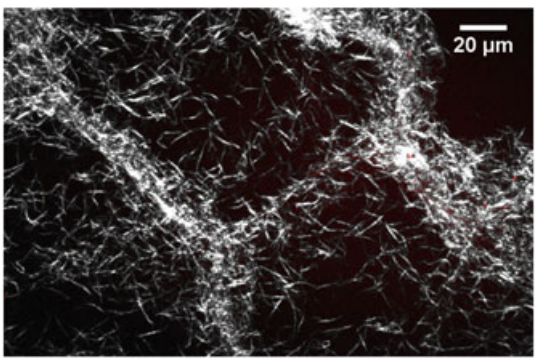

Figure 1. Combined CARS and SHG imaging of a fibrin hydrogel scaffold spiked with 1 mg/mL of rat tail type I collagen. CARS fibrin hydrogel Raman-active band around 2844 cm^{-1} (red signal), SH signal generated by collagen (white signal). This figure is available in colour online at wileyonlinelibrary.com/journal/jrs.

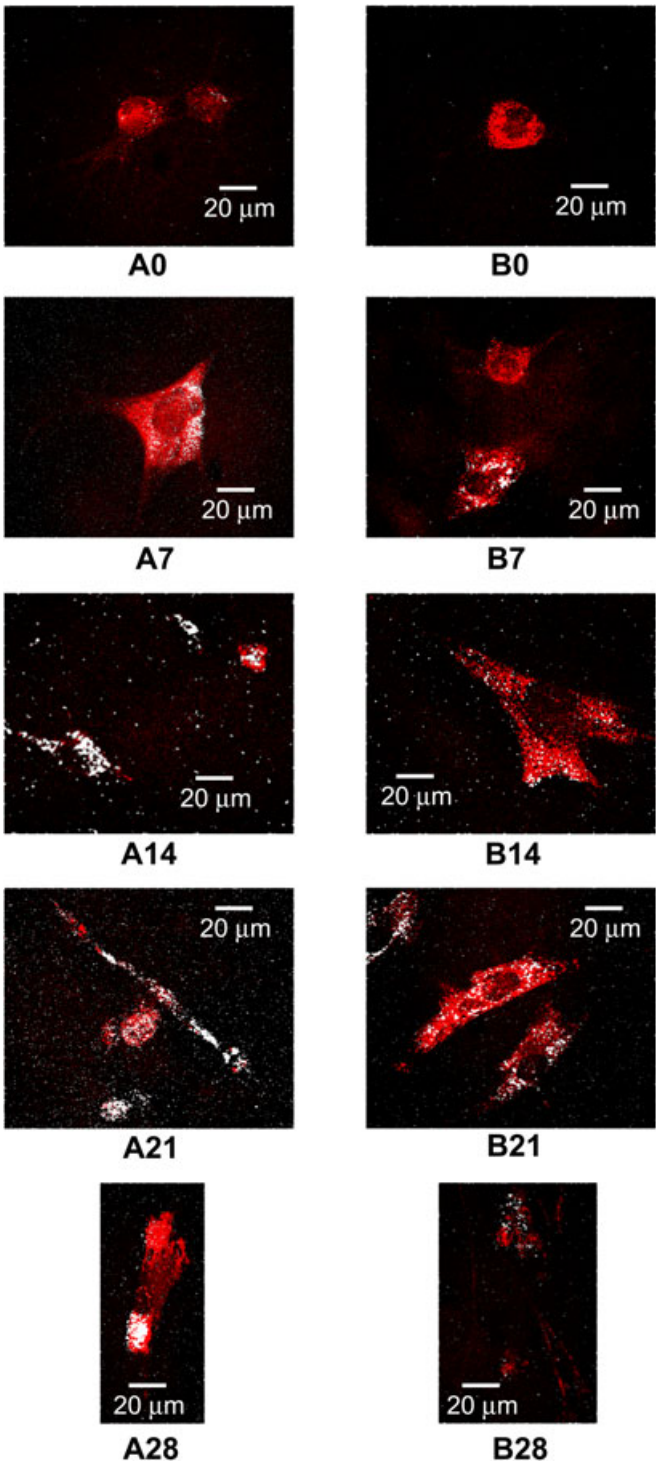

Figure 2. Living human corneal fibroblast (A) and human mesenchymal stem cells (B) morphology in a 4-mm-thick fibrin hydrogel scaffolds (3D CARS imaging in red) and their collagen production (3D SHG imaging in white) at different days in culture (day 0, 7, 14, 21, 28). This figure is available in colour online at wileyonlinelibrary.com/journal/jrs.

In each figure the image (A) refer to hCFs behaviour while the image (B) refer to hMSCs behaviour.

The analysis of the obtained images shows a good cell morphology resolution even if acquired in very thick 3D fibrin hydrogel scaffolds. Cell membranes (rich of lipid structures) and lipid droplets inside the cells were clearly visible in CARS images demonstrating the used, simple, CARS scheme as a powerful tool for this application. The region corresponding to the nucleus appears darker than the other cell compartments in every image in Figure 2, because of the much lower density of lipid structures.

The cell morphology changes during the time experiment were tested in different samples. It shows a good reproducibility and indicates the cell 3D shapes totally different from the shape of cells grown in classical two-dimensional cultures. This makes possible specific studies of the interaction of live cells with scaffolds.

Journal of RAMAN SPECTROSCOPY

Looking at the collagen production, the analysis of the obtained images shows, as expected, at culture day 0 irrelevant collagen production both from fibroblasts and from mesenchymal stem cells. Nevertheless, hCFs show a slight initial collagen formation, indicating that the technique has a very low limit of detection and it is able to detect collagen production after only a few hours of culture. This also indicates that for the used SHG detection scheme the eventual two-photon autofluorescence generated from natively fluorescent compounds inside the cells (like NAD(P)H or oxidized flavoproteins) is not an issue for this experiment. Note that spurious white spots in the images outside the cells come from SHG signal enhancement process noise.

Results at day 7 show more relevant collagen production by hCFs (Fig. 2(A7)); the collagen produced is clearly localized. Unexpectedly, some hMSCs cells (Fig. 2(B7)) also begin to produce collagen, clearly indicating an initial formation of the ECM because of early differentiation process. At days 14, 21 and 28 the collagen production increases both for hCFs and for hMSCs cells, mostly in the cells proximity (Figs 2(B14), (B21) and (B28)). In the majority of the acquired images, collagen produced by hCFs and hMSCs is not localized in correspondence of the nuclear region (the darker round shape region generally situated in the center of the cells). This could be read as a further confirmation of the detection of a protein (collagen), only produced in the cell cytoplasm, not in the nucleus.

Because of the fact that images acquired on different analyzed samples are not related to the same cell or sample region, the variations on the distribution of collagen produced by cells at different culture days as shown in Fig. 2 are not comparable. However, it is possible to confirm the formation of the collagen ECM induced by the fibrin gel scaffold on hMSCs after the 7th day in culture. This result is particularly interesting because it is obtained in unperturbed conditions.

Conclusion

This work demonstrated the multimodal CARS and SHG microscopy as a powerful noninvasive label-free technique to follow the collagen production in living cell 3D cultures. Its ability to image the cell morphology and the produced collagen distribution quite simultaneously on the same sample, on a long term (4 weeks) experiment allowed obtaining important information about the cell–scaffold interaction and the ECM production. The very low limit reached in detecting collagen has permitted to map even the small amount of collagen produced by the cells in a few hours of culture. This demonstrates multimodal CARS and SHG microscopy as a novel method to follow cell collagen production and cell differentiation process in both short-term and long-term experiments. In addition the experiment shows that the technique is a powerful tool for imaging of very thick sections (about 4 mm) with several advantages in its applications. Because collagen production is considered a biomarker for ECM production and also a signal of initial stem cells differentiation, the study conducted on mesenchymal stem cell in 3D cultures confirmed that differentiation stimulus is induced by the fibrin gel scaffold.

The results of this work open new perspectives for tissue engineering and regenerative medicine to investigate rapidly and in a noninvasive way living cell cultures, enabling a better understanding of the interaction between cells and scaffolds and to detect early ECM formation, in the initial stages of the stem cells fibroblastic, chondrogenic and osteogenic differentiation processes. This technique offers advantages to characterize and to evaluate the performance of the cell-ECM/scaffold constructs before implanting them into the donor in preclinical and clinical applications of regenerative medicine.

Acknowledgements

The authors would like to thank Dr Sizzano of the Transplants Centre of the Regione Piemonte for providing the hCFs used in this work. This work was partially supported by Regione Piemonte CIPE 2007 Converging technology Project Metregen - Grant Agreement 0126000010.

References

[1] J. Ringe, C. Kaps, G. Burmester, M. Sittinger, *Naturwissenschaften* **2002**, *89*, 338–351.
[2] H. Shin, S. Jo, A. G. Mikos, *Biomaterials* **2003**, *24*(24), 4353–4364.
[3] A. I. Caplan, *J. Cell. Physiol.* **2007**, *213*, 341–347.
[4] S. J. Forbes, P. Vig, R. Poulsom, N. A. Wright, M. R. Alison, *Clinical Scienc.* **2002**, *103*, 355–369.
[5] G. Chamberlain, J. Fox, B. Ashton, J. Middleton, *Stem Cells* **2007**, *25*, 2739–2749.
[6] Z. Liu, Y. Zhuge, O. C. Velazquez, *J. Cell. Biochem.* **2009**, *106*, 984–991.
[7] P. Lennon, A. I. Caplan, *Exp. Hematol.* **2006**, *34*, 1604–1605.
[8] M. Dominici, K. Le Blanc, I. Mueller, I. Slaper-Cortenbach, F. Marini, D. Krause, R. Deans, A. Keating, D. Prockop, E. Horwitz, *Cytotherapy* **2006**, *8*, 315–317.
[9] M. F. Pittenger, A. M. Mackay, S. C. Beck, R. K. Jaiswal, R. Douglas, J. D. Mosca, M. A. Moorman, D. W. Simonetti, S. Craig, D. R. Marshak, *Science* **1999**, *284*, 143–147.
[10] R. G. M. Bruels, T. U. Jiya, T. H. Smit, *The Open Othopeadic Journal.* **2008**, *2*, 103–109.
[11] D. E. Discher, P. Janmey, Y. Wang, *Science* **2005**, *310*(5751), 1139–1143.
[12] A. J. Engler, S. Sen, H. L. Sweeney, D. E. Discher, *Cell* **2006**, *126*, 677–689.
[13] H. Duong, B. Wu, B. Tawil, *Tissue Eng. Part A* **2009**, *15*(7), 1865–1876.
[14] W. P. Daley, S. B. Peters, M. Larsen, *J. Cell Sci.* **2007**, *121*, 255–264.
[15] D. Pelaez, C. C. Huang, H. S. Cheung, *Stem Cells Dev.* **2009**, *18*(1), 93–102.
[16] R. Hass, C. Kasper, S. Bohm, R. Jacobs, *Cell Communication and Signaling.* **2011**, *9*, 12–26.
[17] M. Jager, T. Feser, H. Denck, R. Krauspe, *Ann. Biomed. Eng.* **2005**, *33*, 1319–1332.
[18] R. T. Franceschi, B. S. Iyer, *J. Bone Miner. Res.* **1992**, *7*(2), 235–246.
[19] L. A. Solchaga, K. J. Penik, J. F. Welter, *Methods Mol. Biol.* **2011**, *698*, 253–278.
[20] Y. Zhou1, X. Guan, Z. Zhu, S. Gao, C. Zhang, C. Li, K. Zhou, W. Hou, H. Yu, *Eur. Cell. Mater.* **2011**, *22*, 12–25.
[21] J. George, Y. Kuboki, T. Miyata, *Biotechnol. Bioeng.* **2006**, *95*(3), 404–411.
[22] G. Cox, E. Kable, A. Jones, I. Fraser, F. Manconi, M. D. Gorrellc, *J. Struct. Biol.* **2003**, *141*, 53–62.
[23] P. A. Janmey, J. P. Winer, J. W. Weisel, *J. R. Soc. Interface* **2009**, *6*, 1–10.
[24] F. Djouad, B. Delorme, M. Maurice, C. Bony, F. Apparailly, P. Louis-Plence, F. Canovas, P. Charbord, D. Noël, C. Jorgensen, *Arthritis Res. Ther.* **2007**, *9*(2), R33.
[25] I. Catelas, N. Sese, B. M. Wu, J. C. Y. Dunn, S. Helgerson, B. Tawil, *Tissue Eng.* **2006**, *12*(8), 2385–2396.
[26] T. Nishida, A. Ueda, M. Fukuda, H. Mishina, K. Yasumoto, T. Otori, *In Vitro Cellular & Development Biology.* **1988**, *24*(10), 1009–1014.

[27] W. R. Zipfel, R. M. Williams, W. W. Webb, *Nat. Biotechnol.* **2003**, *21*(11), 1369–1377.
[28] W. Denk, J. H. Strickler, W. W. Webb, *Science* **1990**, *248*, 73–76.
[29] A. Zumbusch, G.R. Holtom, X. S. Xie, *Phys. Rev. Lett.* **1999**, *82*(20), 4142–4145.
[30] J. Cheng, Y. K. Jia, G. Zheng, X. S. Xie, *Biophys. J.* **2002**, *83*, 502–509.
[31] X. Nan, J. Cheng, X. S. Xie, *Lipid Res.* **2003**, *44*, 2202–2208.
[32] A. Zoumi, A. Yeh, B. J. Tromberg, *PNAS.* **2002**, *99*(17), 11014–11019.
[33] G. Cox, E. Kable, A. Jones, I. Fraser, F. Manconi, M. D. Gorrellc, *J. Struct. Biol.* **2003**, *141*, 53–62.
[34] P. Stoller, P. M. Celliers, K. M. Reiser, A. M. Rubenchik, *Appl. Opt.* **2003**, *42*(25), 5209–5219.
[35] J. Chen, A. Lee, J. Zhao, H. Wang, H. Lui, D. I. McLean, H. Zeng, *Skin Res. Technol.* **2009**, *15*, 418–426.
[36] T. Luo, J. X. Chen, S. M. Zhuo, K. C. Lu, X. S. Jiang, Q. G. Liu, *Laser Physics.* **2009**, *19*(3), 478–482.
[37] R. M. Williams, W. R. Zipfel, W. W. Webb, *Biophys. J.* **2005**, *88*, 1377–1386.
[38] P. Su, W. Chen, T. Li, C. Chou, T. Chen, Y. Ho, C. Huang, S. Chang, Y. Huang, H. Lee, C. Dong, *Biomaterials* **2010**, *31*(36), 9415–21.
[39] P. J. Campagnola, A. C. Millard, M. Terasaki, P. E. Hoppe, C. J. Malone, W. A. Mohler, *Biophys. J.* **2002**, *81*, 493–508.
[40] S. V. Plotnikov, A. C. Millard, P. J. Campagnola, W. A. Mohler, *Biophys. J.* **2006**, *90*(2), 693–703.
[41] C. P. Pfeffer, B. R. Olsen, F. Ganikhanov, F. Légaré, *J. Struct. Biol.* **2008**, *164*(1), 140–145.
[42] P. J. Campagnola, H. A. Clark, W. A. Mohler, A. Lewis, L. M. Loew, *J. Biomed. Opt.* **2001**, *6*(3), 277–286.
[43] C. Brackmann, A. Bodin, M. Åkeson, P. Gatenholm, A. Enejder, *Biomacromolecules* **2010**, *11*, 542–548.
[44] A. D. Slepkov, A. Ridsdale, A. F. Pegoraro, D. J. Moffatt, A. Stolow, *Biomedical Optics Express.* **2010**, *1*(5), 1347–1357.
[45] R. S. Lim, A. Kratzer, N. P. Barry, S. Miyazaki-Anzai, M. Miyazaki, W. W. Mantulin, M. Levi, E. O. Potma, B. J. Tromberg, *J. Lipid Res.* **2010**, *51*, 1729–1737.
[46] A. C. T. Ko, A. Ridsdale, M. S. D. Smith, L. B. Mostaço-Guidolin, M. D. Hewko, A. F. Pegoraro, E. K. Kohlenberg, B. Schattka, M. Shiomi, A. Stolow, M. G. Sowa, *J. Biomed. Opt.* **2010**, *15*(2), 020501.